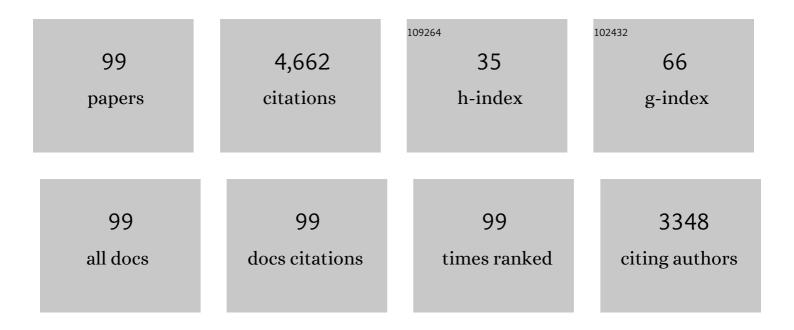
List of Publications by Year in descending order

Source: https://exaly.com/author-pdf/6607081/publications.pdf Version: 2024-02-01



#	Article	IF	CITATIONS
1	Evidence for oxygenic photosynthesis half a billion years before the Great Oxidation Event. Nature Geoscience, 2014, 7, 283-286.	5.4	444
2	Rare Earth Element and yttrium compositions of Archean and Paleoproterozoic Fe formations revisited: New perspectives on the significance and mechanisms of deposition. Geochimica Et Cosmochimica Acta, 2010, 74, 6387-6405.	1.6	373
3	Geodynamo, Solar Wind, and Magnetopause 3.4 to 3.45 Billion Years Ago. Science, 2010, 327, 1238-1240.	6.0	256
4	The geochemistry of sedimentary rocks from the Fig Tree Group, Barberton greenstone belt: Implications for tectonic, hydrothermal and surface processes during mid-Archaean times. Precambrian Research, 2005, 143, 23-49.	1.2	187
5	Sulfur record of rising and falling marine oxygen and sulfate levels during the Lomagundi event. Proceedings of the National Academy of Sciences of the United States of America, 2012, 109, 18300-18305.	3.3	174
6	Titanium isotopic evidence for felsic crust and plate tectonics 3.5 billion years ago. Science, 2017, 357, 1271-1274.	6.0	166
7	Silica alteration zones in the Barberton greenstone belt: A window into subseafloor processes 3.5–3.3ÂGa ago. Chemical Geology, 2008, 257, 221-239.	1.4	157
8	Towards a complete magmatic barcode for the Zimbabwe craton: Baddeleyite U–Pb dating of regional dolerite dyke swarms and sill complexes. Precambrian Research, 2010, 183, 388-398.	1.2	148
9	Iron isotope composition of some Archean and Proterozoic iron formations. Geochimica Et Cosmochimica Acta, 2012, 80, 158-169.	1.6	147
10	Multiple sulphur and iron isotope composition of detrital pyrite in Archaean sedimentary rocks: A new tool for provenance analysis. Earth and Planetary Science Letters, 2009, 286, 436-445.	1.8	113
11	Carbonaceous Cherts in the Barberton Greenstone Belt and Their Significance for the Study of Early Life in the Archean Record. Astrobiology, 2007, 7, 355-388.	1.5	99
12	Coupled Fe and S isotope variations in pyrite nodules from Archean shale. Earth and Planetary Science Letters, 2014, 392, 67-79.	1.8	86
13	Isotopic evidence for oxygenated Mesoarchaean shallow oceans. Nature Geoscience, 2018, 11, 133-138.	5.4	86
14	Generation of early Archaean grey gneisses through melting of older crust in the eastern Kaapvaal craton, southern Africa. Precambrian Research, 2014, 255, 823-846.	1.2	84
15	Microbial remains in some earliest Earth rocks: Comparison with a potential modern analogue. Precambrian Research, 2008, 164, 187-200.	1.2	82
16	Implications of in situ calcification for photosynthesis in a ~3.3Ga-old microbial biofilm from the Barberton greenstone belt, South Africa. Earth and Planetary Science Letters, 2011, 310, 468-479.	1.8	75
17	A trace element and Pb isotopic investigation into the provenance and deposition of stromatolitic carbonates, ironstones and associated shales of the â^1⁄43.0 Ga Pongola Supergroup, Kaapvaal Craton. Geochimica Et Cosmochimica Acta, 2015, 158, 57-78.	1.6	70
18	Cyclicity of Triassic to Lower Jurassic continental red beds of the Argana Valley, Morocco: implications for palaeoclimate and basin evolution. Palaeogeography, Palaeoclimatology, Palaeoecology, 2000, 161, 229-266.	1.0	65

#	Article	lF	CITATIONS
19	The geochemistry of Archaean shales derived from a Mafic volcanic sequence, Belingwe greenstone belt, Zimbabwe: provenance, source area unroofing and submarine versus subaerial weathering. Geochimica Et Cosmochimica Acta, 2003, 67, 421-440.	1.6	64
20	Dykes of the 1.11Ga Umkondo LIP, Southern Africa: Clues to a complex plumbing system. Precambrian Research, 2014, 249, 129-143.	1.2	60
21	Source composition, fractional crystallization and magma mixing processes in the 3.48–3.43Ga Tsawela tonalite suite (Ancient Gneiss Complex, Swaziland) – Implications for Palaeoarchaean geodynamics. Precambrian Research, 2016, 276, 43-66.	1.2	58
22	Two-step deoxygenation at the end of the Paleoproterozoic Lomagundi Event. Earth and Planetary Science Letters, 2018, 486, 70-83.	1.8	58
23	Comparing orthomagmatic and hydrothermal mineralization models for komatiite-hosted nickel deposits in Zimbabwe using multiple-sulfur, iron, and nickel isotope data. Mineralium Deposita, 2014, 49, 75-100.	1.7	56
24	A lithium-isotope perspective on the evolution of carbon and silicon cycles. Nature, 2021, 595, 394-398.	13.7	56
25	Pb- and Nd-isotope systematics of stromatolitic limestones from the 2.7 Ga Ngezi Group of the Belingwe Greenstone Belt: constraints on timing of deposition and provenance. Precambrian Research, 2002, 114, 277-294.	1.2	55
26	Aerobic iron and manganese cycling in a redox-stratified Mesoarchean epicontinental sea. Earth and Planetary Science Letters, 2018, 500, 28-40.	1.8	54
27	A Mesoarchean shift in uranium isotope systematics. Geochimica Et Cosmochimica Acta, 2018, 238, 438-452.	1.6	52
28	Diagenetic xenotime age constraints on the Sanjiaotang Formation, Luoyu Group, southern margin of the North China Craton: Implications for regional stratigraphic correlation and early evolution of eukaryotes. Precambrian Research, 2014, 251, 21-32.	1.2	51
29	A review of Palaeoarchaean felsic volcanism in the eastern Kaapvaal craton: Linking plutonic and volcanic records. Geoscience Frontiers, 2018, 9, 667-688.	4.3	47
30	Early continental crust generated by reworking of basalts variably silicified by seawater. Nature Geoscience, 2019, 12, 769-773.	5.4	45
31	A review of the stratigraphy and geological setting of the Palaeoproterozoic Magondi Supergroup, Zimbabwe – Type locality for the Lomagundi carbon isotope excursion. Precambrian Research, 2010, 182, 254-273.	1.2	44
32	Limited oxygen production in the Mesoarchean ocean. Proceedings of the National Academy of Sciences of the United States of America, 2019, 116, 6647-6652.	3.3	42
33	Evidence for a 3.45â€billionâ€yearâ€old magnetic remanence: Hints of an ancient geodynamo from conglomerates of South Africa. Geochemistry, Geophysics, Geosystems, 2009, 10, .	1.0	40
34	Precise U-Pb baddeleyite age dating of the Usushwana Complex, southern Africa – Implications for the Mesoarchaean magmatic and sedimentological evolution of the Pongola Supergroup, Kaapvaal Craton. Precambrian Research, 2015, 267, 174-185.	1.2	39
35	An atmospheric source of S in Mesoarchaean structurally-controlled gold mineralisation of the Barberton Greenstone Belt. Precambrian Research, 2016, 285, 10-20.	1.2	38
36	Juvenile crust formation in the Zimbabwe Craton deduced from the O-Hf isotopic record of 3.8–3.1 Ga detrital zircons. Geochimica Et Cosmochimica Acta, 2017, 215, 432-446.	1.6	37

#	Article	IF	CITATIONS
37	Chapter 5.5 Silicified Basalts, Bedded Cherts and Other Sea Floor Alteration Phenomena of the 3.4 Ga Nondweni Greenstone Belt, South Africa. Neoproterozoic-Cambrian Tectonics, Global Change and Evolution: A Focus on South Western Gondwana, 2007, 15, 571-605.	0.2	36
38	Trace element zoning of sulfides and quartz at Sheba and Fairview gold mines: Clues to Mesoarchean mineralisation in the Barberton Greenstone Belt, South Africa. Ore Geology Reviews, 2014, 56, 94-114.	1.1	36
39	Unusual manganese enrichment in the Mesoarchean Mozaan Group, Pongola Supergroup, South Africa. Precambrian Research, 2016, 281, 414-433.	1.2	35
40	Analytical requirements for quantitative X-ray fluorescence nano-imaging of metal traces in solid samples. TrAC - Trends in Analytical Chemistry, 2017, 91, 104-111.	5.8	35
41	Cellular remains in a ~3.42-billion-year-old subseafloor hydrothermal environment. Science Advances, 2021, 7, .	4.7	34
42	Exceptional preservation of expandable clay minerals in the ca. 2.1Ga black shales of the Francevillian basin, Gabon and its implication for atmospheric oxygen accumulation. Chemical Geology, 2013, 362, 181-192.	1.4	31
43	Thrust-related accretion of an Archaean greenstone belt in the Midlands of Zimbabwe. Journal of Structural Geology, 2002, 24, 1707-1727.	1.0	29
44	Zircon SHRIMP dating confirms a Palaeoarchaean supracrustal terrain in the southeastern Kaapvaal Craton, southern Africa. Gondwana Research, 2012, 21, 818-828.	3.0	29
45	Differentiating marine vs hydrothermal processes in Devonian carbonatemounds using rare earth elements (Kess Kess mounds, Anti-Atlas, Morocco). Chemical Geology, 2015, 409, 69-86.	1.4	29
46	A paleosol record of the evolution of Cr redox cycling and evidence for an increase in atmospheric oxygen during the Neoproterozoic. Geobiology, 2019, 17, 579-593.	1.1	27
47	Chapter 7 A review of the current status of the Older Metamorphic Group and Older Metamorphic Tonalite Gneiss: insights into the Palaeoarchaean history of the Singhbhum craton, India. Geological Society Memoir, 2015, 43, 103-107.	0.9	26
48	The Nhlangano gneiss dome in south-west Swaziland – A record of crustal destabilization of the eastern Kaapvaal craton in the Neoarchaean. Precambrian Research, 2015, 258, 109-132.	1.2	25
49	Desilication in Archean weathering processes traced by silicon isotopes and Ge/Si ratios. Chemical Geology, 2016, 420, 139-147.	1.4	25
50	<scp>I</scp> ceâ€margin fluctuation sequences and grounding zone wedges: The record of the Late Palaeozoic Ice Age in the eastern Karoo Basin (Dwyka Group, South Africa <scp>)</scp> . Depositional Record, 2019, 5, 247-271.	0.8	24
51	Chromium isotope systematics and the diagenesis of marine carbonates. Earth and Planetary Science Letters, 2021, 562, 116824.	1.8	24
52	3.51ÂGa old felsic volcanic rocks and carbonaceous cherts from the Gorumahisani Greenstone Belt – Insights into the Palaeoarchaean record of the Singhbhum Craton, India. Precambrian Research, 2021, 357, 106109.	1.2	22
53	The Belingwe Greenstone Belt: Ensialic or Oceanic?. Neoproterozoic-Cambrian Tectonics, Global Change and Evolution: A Focus on South Western Gondwana, 2004, , 487-538.	0.2	21
54	Crystallisation of magmatic topaz and implications for Nb–Ta–W mineralisation in F-rich silicic melts — The Ary-Bulak ongonite massif. Lithos, 2014, 202-203, 317-330.	0.6	21

#	Article	IF	CITATIONS
55	Petrochemical characterization of Neoproterozoic Colomine granitoids, SE Cameroon: Implications for gold mineralization. Lithos, 2019, 344-345, 175-192.	0.6	21
56	Diagenetic Fe-carbonates in Paleoarchean felsic sedimentary rocks (Hooggenoeg Formation,) Tj ETQq0 0 0 rgBT budget of seawater. Precambrian Research, 2009, 172, 255-278.	/Overlock 1.2	10 Tf 50 707 20
57	Archean spherule layers in the Barberton greenstone belt, South Africa: A discussion of problems related to the impact interpretation. , 2006, , .		18
58	The Archaean geological history of the Singhbhum Craton, India – a proposal for a consistent framework of craton evolution. Earth-Science Reviews, 2022, 228, 103994.	4.0	18
59	Horizontal tectonic deformation geometries in a late Archaean sedimentary sequence, Belingwe greenstone belt, Zimbabwe. Tectonics, 2001, 20, 909-932.	1.3	17
60	Discovery of extraterrestrial component carrier phases in Archean spherule layers: Implications for estimation of Archean bolide sizes. Geology, 2015, 43, 299-302.	2.0	17
61	3.2 Ga detrital uraninite in the Witwatersrand Basin, South Africa: Evidence of a reducing Archean atmosphere. Geology, 2018, 46, 295-298.	2.0	16
62	Petrogenesis of the Neoarchean diorite-granite association in the Wangwushan area, southern North China Craton: Implications for continental crust evolution. Precambrian Research, 2019, 326, 84-104.	1.2	16
63	Fluid inclusion analysis of silicified Palaeoarchaean oceanic crust – A record of Archaean seawater?. Precambrian Research, 2015, 266, 150-164.	1.2	15
64	The Pongola Supergroup: Mesoarchaean Deposition Following Kaapvaal Craton Stabilization. Regional Geology Reviews, 2019, , 225-254.	1.2	15
65	Archaean Hydrothermal Systems in the Barberton Greenstone Belt and Their Significance as a Habitat for Early Life. , 2011, , 51-78.		15
66	Nondestructive spectroscopic and petrochemical investigations of Paleoarchean spherule layers from the <scp>ICDP</scp> drill core <scp>BARB</scp> 5, Barberton Mountain Land, SouthÂAfrica. Meteoritics and Planetary Science, 2016, 51, 2441-2458.	0.7	14
67	Characterization of kerogenous films and taphonomic modes of the Sirius Passet Lagerstäe, Greenland. Geology, 2018, 46, 359-362.	2.0	14
68	A revised classification scheme of pyrite in the Witwatersrand Basin and application to placer gold deposits. Earth-Science Reviews, 2020, 201, 103064.	4.0	14
69	The onset of deep recycling of supracrustal materials at the Paleo-Mesoarchean boundary. National Science Review, 2022, 9, nwab136.	4.6	14
70	The origin of early continental crust: New clues from coupling Ge/Si ratios with silicon isotopes. Earth and Planetary Science Letters, 2022, 582, 117415.	1.8	14
71	Uranium isotope evidence for Mesoarchean biological oxygen production in shallow marine and continental settings. Earth and Planetary Science Letters, 2020, 551, 116583.	1.8	13
72	Coupled stable chromium and iron isotopic fractionation tracing magmatic mineral crystallization in Archean komatiite-tholeiite suites. Chemical Geology, 2021, 576, 120121.	1.4	12

AXEL HOFMANN

#	Article	IF	CITATIONS
73	Age of the Dominion-Nsuze Igneous Province, the first intracratonic Igneous Province of the Kaapvaal Craton. Precambrian Research, 2021, 363, 106335.	1.2	12
74	Gold mobility during Palaeoarchaean submarine alteration. Earth and Planetary Science Letters, 2017, 462, 47-54.	1.8	11
75	The Mesoarchaean Dominion Group and the onset of intracontinental volcanism on the Kaapvaal craton – Geological, geochemical and temporal constraints. Gondwana Research, 2020, 84, 131-150.	3.0	11
76	Anoxic continental surface weathering recorded by the 2.95†Ga Denny Dalton Paleosol (Pongola) Tj ETQq0 C	0 rgBT /0\ 1.6	verlock 10 Tf 5
77	Geology, zircon U–Pb dating and εHf data for the Julie greenstone belt and associated rocks in NW Ghana: Implications for Birimian-to-Tarkwaian correlation and crustal evolution. Journal of African Earth Sciences, 2022, 186, 104444.	0.9	11
78	Archaean Granitoid–Greenstone Geology of the Southeastern Part of the Kaapvaal Craton. Regional Geology Reviews, 2019, , 33-54.	1.2	10
79	Palaeoarchaean felsic magmatism: A melt inclusion study of 3.45 Ga old rhyolites from the Barberton Greenstone Belt, South Africa. Chemical Geology, 2015, 414, 69-83.	1.4	9
80	Hydrothermal clay mineral formation in the uraniferous Paleoproterozoic FA Formation, Francevillian basin, Gabon. Precambrian Research, 2014, 246, 134-149.	1.2	8
81	Petrographic and Micro-XRF analysis of multiple archean impact-derived spherule layers in drill core CT3 from the northern Barberton Greenstone Belt (South Africa). Journal of African Earth Sciences, 2018, 138, 264-288.	0.9	8
82	The Late Palaeozoic Ice Age unconformity in southern Namibia viewed as a patchwork mosaic. Depositional Record, 2022, 8, 419-435.	0.8	8
83	Mesoarchaean Gold Mineralisation in the Barberton Greenstone Belt: A Review. Regional Geology Reviews, 2019, , 171-184.	1.2	7
84	High-grade metamorphism of ironstones in the Mesoarchaean of southwest Swaziland. Mineralogy and Petrology, 2014, 108, 589-605.	0.4	6
85	Hafnium-Neodymium isotope, trace element and U-Pb zircon age constraints on the petrogenesis of the 3.44–3.46ÂGa Dwalile greenstone remnant, Ancient gneiss Complex, Swaziland. Precambrian Research, 2020, 351, 105970.	1.2	6
86	Constraining provenance for the uraniferous Paleoproterozoic Francevillian Group sediments (Gabon) with detrital zircon geochronology and geochemistry. Precambrian Research, 2020, 343, 105724.	1.2	6
87	Mesoarchaean acidic volcanic lakes: A critical ecological niche in early land colonisation. Earth and Planetary Science Letters, 2021, 556, 116725.	1.8	6
88	Continental extensional setting for the Archean Belingwe Greenstone Belt, Zimbabwe: Comment and Reply. Geology, 1999, 27, 667.	2.0	5
89	Continental setting inferred for emplacement of the 2.9–2.7 Ga Belingwe Greenstone Belt, Zimbabwe: Comment and Reply. Geology, 2003, 31, e30-e31.	2.0	4
90	(Ca-Y)-phosphate inclusions in apatite crystals from Archean rocks from the Barberton Greenstone Belt and Pilbara Craton: First report of natural occurrence. American Mineralogist, 2018, 103, 307-313.	0.9	4

#	Article	IF	CITATIONS
91	The Paleoarchean Record of the Zimbabwe Craton. , 2019, , 855-864.		4
92	Possible discontinuous evolution of atmospheric xenon suggested by Archean barites. Chemical Geology, 2021, 581, 120405.	1.4	4
93	Reply to the comment by Préat and Weber on. Earth and Planetary Science Letters, 2019, 511, 259-261.	1.8	3
94	Limited expression of the Paleoproterozoic Oklo natural nuclear reactor phenomenon in the aftermath of a widespread deoxygenation event ~2.11–2.06 billion years ago. Chemical Geology, 2021, 578, 120315.	1.4	3
95	2470 million-year-old banded iron formation reveals a climatic oscillation consistent with the Gleissberg solar cycle. Communications Earth & Environment, 2022, 3, .	2.6	3
96	Crustal modelling from Pan-African granites of the Colomine Gold District, SE Cameroon: Insights from zircon U-Pb dating and Lu-Hf isotope systematics. Journal of African Earth Sciences, 2022, 187, 104441.	0.9	2
97	Barberton Greenstone Belt, Sedimentology. , 2014, , 1-3.		0
98	Barberton Greenstone Belt, Sedimentology. , 2015, , 244-246.		0
99	Barberton Greenstone Belt, Sedimentology. , 2021, , 1-3.		0